Title: Medial prefrontal-medial temporal theta phase coupling in dynamic spatial imagery

Abbreviated Title: mPFC-MTL theta phase coupling in dynamic imagery

Authors: Raphael Kaplan[1,2,3]*, Daniel Bush[1,4]*, James A Bisby[1,4], Aidan J Horner[1,5], Sofie S Meyer[1,2], Neil Burgess[1,4]

Author Affiliations:
1-UCL Institute of Cognitive Neuroscience, University College London, Alexandra House, 17 Queen Square, London, United Kingdom WC1N 3AZ
2-Wellcome Trust Centre for Neuroimaging, UCL Institute of Neurology, University College London, 12 Queen Square, London, United Kingdom WC1N 3BG
3-Center for Brain and Cognition, Departament de Tecnologies de la Informacio I les Comunicacions, Universitat Pompeu Fabra, Barcelona, Spain 08001.
4-UCL Institute of Neurology, University College London, United Kingdom WC1N 3AZ
5 – Department of Psychology, University of York, United Kingdom YO10 5DD

*=authors contributed equally to the manuscript

Corresponding Authors: Raphael Kaplan and Neil Burgess; email: raphael.kaplan@upf.edu, Wellcome Trust Centre for Neuroimaging, UCL Institute of Neurology, University College London, 12 Queen Square, London, United Kingdom WC1N 3BG; n.burgess@ucl.ac.uk; UCL Institute of Cognitive Neuroscience; Alexandra House, 17 Queen Square; London, WC1N 3AZ United Kingdom

Conflict of Interest: The authors declare no competing financial interests.

Acknowledgements: The research was supported by a Sir Henry Wellcome Postdoctoral Fellowship (WT101261MA) to RK, Medical Research Council UK and Wellcome Trust grants to NB, and an MRC Doctoral Training Grant (MR/K501086/1) to SSM. The authors would like to thank Gareth Barnes for helpful discussion and Letty Manyande for help with scanning. The Wellcome Trust Centre for Neuroimaging is supported by core funding from the Wellcome Trust 091593/Z/10/Z. The authors declare no competing financial interests.

Abstract

Hippocampal-medial prefrontal interactions are thought to play a crucial role in mental simulation. Notably, the frontal midline / medial prefrontal cortex (mPFC) theta rhythm in humans has been linked to introspective thought and working memory. In parallel, theta rhythms have been proposed to coordinate processing in medial temporal, retrosplenial and parietal cortices during the movement of viewpoint in imagery, extending their association with physical movement in rodent models. Here, we used non-invasive whole-head magnetoencephalography (MEG) to investigate theta oscillatory power and phase-locking during the 18s post-encoding delay period of a spatial working memory task, in which participants imagined previously learned object sequences either: on a blank background (object maintenance); from a first person viewpoint in a scene (static imagery); or moving along a path past the objects (dynamic imagery). We found increases in 4-7 Hz theta power in mPFC when comparing the delay period to a pre-encoding baseline. We then examined whether the mPFC theta rhythm was phase coupled with ongoing theta oscillations elsewhere in the brain. The same mPFC region showed significantly higher theta phase coupling with the posterior medial temporal lobe / retrosplenial cortex (MTL/RSc) for dynamic imagery versus either object maintenance or static imagery. mPFC theta phase coupling was not observed with any other brain region. These results implicate oscillatory coupling between mPFC and MTL / RSc theta rhythms in the dynamic mental exploration of imagined scenes.

Introduction

Our capacity to imagine spatially cohesive representations is associated with the medial prefrontal cortex (mPFC) and medial temporal lobe (MTL) regions such as the hippocampus (Burgess et al., 2001; Hassabis et al., 2007; Addis & Schacter 2008; Schacter et al., 2012). Increases in ~4-8 Hz mPFC oscillatory power, known as the frontal midline theta rhythm, are observed during internally generated behaviors such as abstract thinking and meditation (Banquet, 1973; Lehmann et al., 1993; Sasaki et al., 1996; Aftanas & Golochelkine, 2001). Notably, there is growing evidence that the frontal midline theta rhythm is also implicated in working and episodic memory function (see Hsieh & Ranganath, 2014 for a recent review).

In parallel, hippocampal theta oscillations in the medial temporal lobe (MTL) have been hypothesized to serve as a network hub (Battaglia et al., 2011) and global signal integrator (O'Keefe, 2006) for information from neocortical regions, including the mPFC and medial parietal / retrosplenial (RSc) cortices. The hippocampal theta rhythm is strongly associated with translational movement in rodents (Vanderwolf, 1969; O'Keefe & Nadel, 1978), but has also been observed in the human MTL and several neocortical areas including the mPFC and the medial parietal lobe / RSc during virtual navigation (Kahana et al., 1999; Caplan et al., 2003; Ekstrom et al., 2005; Kaplan et al., 2012). Recently, several studies have found increased theta phase coupling between these regions during spatial and autobiographical memory retrieval (Foster et al., 2013; Watrous et al., 2013; Fuentemilla et al., 2014; Kaplan et al., 2014), but whether theta power or phase coupling contributes to spatial imagery is currently unclear.

This issue is addressed by a speculative neural-level model of memory guided

visuo-spatial imagery (Burgess et al., 2001; Byrne et al., 2007; Bird & Burgess, 2008). It proposes that the MTL provides allocentric scene information consistent with a single viewpoint location, and that this information is translated, via intermediate representations in RSc, into an egocentric image consistent with a specific viewing direction, supported in a medial parietal 'window' (PW). This 'top-down' activation of the PW from MTL occurs during the first half of each theta cycle, while 'bottom-up' updating of the MTL representation from the PW representation occurs in the second half of each cycle – allowing egocentric manipulations in the PW to propagate back to the MTL. These egocentric manipulations include selective attention to specific scene elements (allowing reactivation of their identity / perceptual properties in the MTL), and spatial updating due to real or imagined movement of viewpoint.

According to this model, during actual movement, at the start of a theta cycle, motor efference copy from premotor areas (Graziano & Gross, 1993) drives egocentric spatial updating of locations by modifying the allocentric to egocentric translation to accommodate the effect of the movement. The updated egocentric representation then feeds back to update MTL representations during the second half of the theta cycle. The model proposes that imagined movement of viewpoint (dynamic imagery) occurs in the same way, driven by mock motor-efference copy from prefrontal cortex, which could be used in behaviors like planning. The theta rhythmicity associated with prefrontal control of working memory maintenance (Hsieh & Ranganath, 2014) would thus have to synchronize with the theta-modulated MTL-PW interaction so as to be able to direct dynamic imagery. However, we are unaware of any attempts to investigate theta rhythmicity or phase coupling during dynamic imagery.

Using a spatial working memory task with non-invasive whole-head

magnetoencephalography (MEG), we tested this prediction. In the experiment, participants encoded the location of five objects overlaid on a scene or blank background (Fig. 1). Participants then closed their eyes during a 20s eyes-closed delay period and imagined previously learned object sequences either: overlaid on a blank background (object maintenance, Fig. 1A); from a static first-person viewpoint in a scene (static imagery, Fig. 1B); or moving along a path past the objects (dynamic imagery, Fig. 1C). Afterwards, participants were prompted to sequentially match each object to its respective location on the screen, in the scene or along the path.

We were primarily interested in the potential co-occurrence of frontal midline / mPFC, RSc, and MTL theta oscillations, inter-regional mPFC theta phase coupling during the delay period, and whether these phenomena would be modulated by the context of the object-sequence imagination task (blank, static spatial or dynamic spatial). We predicted an increase in frontal midline / mPFC theta power during the delay period, due to the demands of working memory function (Hsieh & Ranganath, 2014). In addition, theta phase coupling with MTL and parietal regions, indicating the presence of functional interactions between these regions, would be specifically recruited to dynamically shift viewpoint during spatial imagery. The blank background condition provides a necessary control for the basic working memory components of the task, while the static imagery condition provides a control for working memory accompanied by spatial imagery in the absence of imagined movement. Although spatial updating of object locations could be performed egocentrically (Wang and Simons, 1999; Wang and Spelke, 2000), in the context of a spatial scene the updating of object locations also involves allocentric processing of locations relative to the environment (Burgess et al., 2004) and thus egocentric-allocentric translation (Burgess, 2006). Thus we predicted

that mPFC-MTL / parietal theta phase-locking would specifically increase with dynamic imagery demands.

Methods

Participants

Sixteen participants (7 female; mean age of 22.8 years; SD of 4.07 years) gave written consent and were compensated for performing the experimental task, as approved by the local research ethics committee at University College London in accordance with Declaration of Helsinki protocols. All participants were right-handed, had normal or corrected-to-normal vision and reported to be in good health with no prior history of drug abuse, neurological disease, or psychiatric illness.

Task

Stimuli were presented via a digital LCD projector (brightness: 1500 lumens; resolution: 1024 x 768 pixels; refresh rate: 60 Hz) onto a screen (height: 32 cm; width: 42 cm; distance from participant: ~70 cm) that was parallel to the participant's face inside a magnetically shielded room using the Cogent (http://www.vislab.ucl.ac.uk/cogent.php) toolbox running in MATLAB (Mathworks, Natick, MA, USA). Participants were fitted with MEG compatible earbuds to deliver auditory stimuli associated with the experiment.

Participants performed a spatial working memory task in the MEG system, during which they were asked to remember the locations of five different everyday objects (e.g. bicycle, lemon, etc.) framed by an equally sized white square and overlaid

on a blank background or scene. Participants first viewed an example video of each condition recorded from a first-person viewpoint with the same sequence of objects, so they would have an idea of what to imagine and the ideal pacing of imagination during each particular delay period. Participants were instructed to repeat imagination of the sequences if they finished imagining a learned sequence before the end of the delay period. Participants then performed a single practice session of the task, before three counterbalanced pseudo-randomized sessions lasting approximately 15 minutes each inside the scanner.

In the task, participants first had a 20s baseline period of eyes closed rest. This was followed by a 3s habituation period, during which participants viewed either a blank background or one of four different scenes created using Unity software (Unity Technologies). A different scene was used for each session (dirt surface environment containing a cemetery and small river with a bridge; grassy forest clearing containing walking paths and a church; a beach environment with tents and stranded boats; and, for the practice session, a grassy hill environment containing a small pond and castle). Each scene had a bench in the foreground. After the end of the habituation period, participants were sequentially presented with five objects, arranged circularly in different locations over the scene / background. Each new object was highlighted with a red frame and would appear for three seconds (with a randomized +/- .3 second jitter) until all objects appeared overlaid on the background. The appearance of each new object was preceded by a blink period, during which the objects and scene were replaced with a fixation point and the word BLINK for one second. This was followed by a two second inter-trial interval before the object sequence resumed with another object highlighted with a red frame. Blocks were counterbalanced for starting location

and direction of object presentation (clockwise and counter-clockwise). Objects were presented either in a larger circle, to give way for a plausible walking path for dynamic imagery; or were clustered in a small circle in front of a bench in the foreground in order for all objects to be visible from a single viewpoint inside the environment. For the object maintenance condition, objects were presented with equal frequency in either large or small circles over a black background. Importantly, there were no significant differences in behavioural memory performance ($t(15)=.011$; $p=.992$); reaction times ($t(15)=-1.34$, $p=.198$); subjective memory ($t(15)=.983$, $p=.341$); or vividness ratings ($t(15)=.433$, $p=.671$) between trials with objects arranged in large and small circles within this condition.

After the encoding phase of the experiment, participants had a 20-s delay period. During the delay period, participants received instructions to close their eyes and either: imagine sitting and passively viewing the locations of the objects in the scene from a static position on the bench (static imagery); imagine walking slowly through the scene, passing each object sequentially (dynamic imagery); or, in the case of objects being presented over a black background, simply to 'remember the locations of the objects' (object maintenance). They were cued to open their eyes with an auditory tone played into the participants' headphones.

After the auditory tone, the scene / black background from the encoding period was presented again with numbered squares (1-5) superimposed in place of the objects. Participants were then prompted with a picture of each object at the top of the screen and had to match the object to the number of its corresponding location at their own pace. Immediately following the matching of the spatial location for each object, participants had to indicate how good their memory was for that block and how vivid

their imagination during the delay period had been on a 1-5 scale, with one being very low and five being very high.

Participants performed a total of 36 blocks across three sessions, with each of the three conditions being pseudo-randomized within a session. Scene order was also counterbalanced across participants. Over the course of the MEG experiment, participants learned twelve different sequences of objects (sixty objects in total), once for each of the three conditions and counterbalanced for order.

MEG recording and preprocessing

Data were recorded continuously from 274 axial gradiometers using a CTF Omega whole-head system at a sampling rate of 600 Hz in third-order gradient configuration. MEG was preferred to EEG in this experiment due to the increased number of recording channels, high signal-to noise ratio, and reduced set-up time. Participants were also fitted with four electrooculargram (EOG) electrodes to measure vertical and horizontal eye movements. MEG data analysis made use of custom Matlab scripts, SPM8 (Wellcome Trust Centre for Neuroimaging, London; Litvak et al., 2011) and Fieldtrip (Oostenveld et al., 2011).

For preprocessing, MEG data was epoched into 20s baseline periods prior to the encoding period and during the delay period for each of the three conditions. Trials were visually inspected, with any trial featuring head movement or muscular artefacts being removed, along with any corresponding baseline or task period to allow for consistent trial comparison. After visual inspection, a mean of 32.1 trials (SD=6.04) from the total of 36 trials in the experiment remained for analysis. This included a mean of 10.7 dynamic imagery trials (SD=2.5), 10.6 static imagery trials (SD=2.19), and 10.8

object maintenance trials (SD=1.8) per participant, regardless of trial by trial performance. In order to avoid further physiological artefacts, data was not analysed until one second after the beginning of eyes closed maintenance or baseline period and not until one second before the end (i.e. the central 18s of the 20s delay period).

MEG Source Reconstruction

The linearly constrained minimum variance (LCMV) scalar beamformer spatial filter algorithm from SPM8 was applied to the raw time series and used to generate source activity maps in a 10-mm grid (Barnes et al., 2003). Coregistration to MNI coordinates was based on nasion, left and right preauricular fiducial points. The forward model was derived from a single-shell model (Nolte, 2003) fit to the inner skull surface of the inverse normalized SPM template. Previous studies have shown negligible improvements in spatial resolution by fitting MEG data to individual structural MR images, rather than a canonical template image, under realistic levels of error and head movement (Henson et al., 2009; Troebinger et al., 2014). The beamformer source reconstruction algorithm consists of two stages: first, based on the data covariance and leadfield structure, weights are calculated which linearly map sensor data to each source location; and second, a summary statistic based on the mean oscillatory power between experimental conditions is calculated for each voxel.

Due to the proximity of frontal midline regions to the eyes, we wished to control for any possible influence of EOG muscular artifacts during the maintenance period on estimates of oscillatory power. We therefore computed the variance of two simultaneously recorded EOG signals across each delay period, as a proxy for the number of eye movements made during that delay period, and removed any covariance

between these EOG variance values and oscillatory power measurements across voxels by linear regression (Kaplan et al., 2014). This left 'residual' oscillatory power measurements for all trials whose variance could not be accounted for by changes in the variance of the EOG signal between trials, and these residual values were used as summary images for subsequent analyses.

In addition to movements in the ocular region, phase coupling measures can be biased by concurrent changes in oscillatory power due to changes in the signal to noise ratio (Muthukumaraswamy & Singh, 2011). To control for any possible influence of changes in oscillatory power (or EOG artifacts) on our phase coupling measures, we repeated the control analysis described above, with additional linear regressors corresponding to oscillatory power in seed and source voxels for each trial (Kaplan et al., 2014). Similarly, we constructed linear regressors for four behavioral measures across trials - reaction time, memory performance (percentage of object locations remembered correctly for a given trial), subjective memory, and vividness ratings - to examine correlations between behavioural performance and phase coupling values across trials in each voxel.

Phase Coupling

Instantaneous theta phase in voxel n at time t, Ø(t,n), was extracted from the analytic signal obtained by applying the Hilbert transform to the 4-7 Hz band-pass 2nd order Butterworth filtered time series generated by the LCMV beamformer algorithm. The mPFC seed voxel for each participant was chosen as that with the greatest power increase between baseline and maintenance periods within 20 mm of the group maximum coordinates to account for observed variance in frontal midline source

location between participants (Isihara et al., 1981; Kaplan et al., 2014). Firstly, we used the phase lag index (PLI) to assay theta phase coupling between that single seed voxel and every other voxel in the brain. The PLI is computed by assigning a value of +1 or −1 at each time step according to whether the phase difference between seed and source voxels is positive or negative and then taking the absolute value of the mean over time, which will tend to zero for randomly distributed phase differences and to one for a consistent nonzero phase relationship [Eq. (1)]. The PLI measure is designed to ameliorate volume conduction effects by being increasingly less sensitive to coupling effects as phase differences approach zero (Stam et al., 2007). PLI values for each trial are averaged for each condition before being entered into a second level statistical analysis.

$$PLI = \frac{1}{T}\left|\sum_{t=1}^{T} sign[\emptyset(t, seed) - \emptyset(t, n)]\right|$$

Equation 1: The phase lag index (PLI)

Secondly, to confirm the robustness of our PLI effects, we conducted a parallel phase coupling analysis using the phase locking value (PLV: Lachaux et al., 1999). The PLV is computed as the resultant vector length of phase differences at each time point, such that a larger value indicates less variability in the phase difference between two signals over time [Eq. (2)]. As with PLI values, PLV values for each trial are averaged for each condition before being entered into a second level statistical analysis.

$$PLV = \frac{1}{T}\left|\sum_{t=1}^{T} \exp(i[\emptyset(t, seed) - \emptyset(t, n)])\right|$$

Equation 2: The phase locking value (PLV)

Statistical Analyses

For comparison between delay period and baseline condition, summary images for each participant were entered into a one-sample t-test in SPM8. Regressors for reaction time, memory performance (percentage of object locations remembered correctly for a given trial), subjective memory, and vividness ratings, in addition to the 'nuisance' regressors described above, were each included in the general linear model. For comparisons between conditions, summary images for each participant and each delay period condition (object maintenance, static imagery, and dynamic imagery) were entered into a second level 1x3 within-subjects ANOVA in SPM8.

To address the issue of multiple comparisons, we used family-wise error (FWE) correction, derived from Gaussian Random Field Theory, and implemented in SPM8 (Worsley et al., 1996; Kiebel and Friston, 2004a; Kiebel and Friston, 2004b; Worsley et al., 2004). To summarize, this approach treats the data, under the null hypothesis, as continuous random fields, where the distribution of the Euler characteristic of any statistical process derived from these fields can be used as an approximation to the null distribution required for inference (Kilner et al., 2005). A peak voxel significance threshold of $p<0.05$ FWE corrected for multiple comparisons across the whole brain volume was used for power analyses. For theta phase coupling analyses, an MTL region of interest (ROI) for small-volume correction (SVC) for multiple comparisons (peak voxel FWE $p<0.05$) was constructed using a bilateral MTL mask encompassing the amygdala, hippocampus, parahippocampal, and lingual gyrus (to conservatively include all of parahippocampal place area regions that respond to landmark information;

Epstein, 2008) from the automated anatomical labeling (AAL) toolbox for SPM (Tzourio-Mazoyer et al, 2002). All images are displayed at the $p<0.001$ uncorrected threshold (cluster extent of at least 20 voxels after interpolation to the MNI brain) for illustrative purposes. Additionally, only clusters containing a significant peak voxel are displayed.

Results

Behavioral Results

Participants remembered an average of 74.7% (standard error=5.33%) object locations correctly with a mean reaction time of 1980 ms for matching an individual object to its respective location after the onset of the retrieval period. On a scale of 1-5 (1 being unsatisfactory and 5 being very good), participants rated each working memory trial for subjective vividness (mean=3.37; standard error=0.147) and subjective memory (mean=3.81; standard error=0.167). There was a significant interaction between performance and condition ($F(2,30)=5.66$, $p=.016$; Fig 2A), where performance was significantly higher for object maintenance than static imagery ($t(15)=3.21$; $p=.006$), but not dynamic imagery ($t(15)=.715$; $p=.486$). We observed no significant difference between memory performance in static and dynamic imagery conditions ($t(15)=1.67$; $p=.117$).

During the retrieval period, there was no significant difference in reaction time when matching objects to their location between the three conditions ($F(2,30)=3.30$; $p=0.067$; Fig. 2B). There was, however, a significant difference in subjective memory ratings by condition ($F(2,30)=11.4$; $p=.001$; Fig. 2C). Similar to measured memory performance, subjective memory ratings were significantly higher for object

maintenance than static imagery (t(15)=4.10; p=.001), but not dynamic imagery trials (t(15)=1.54; p=.144). Subjective memory ratings were also higher for dynamic than static imagery trials (t(15)=2.58; p=.021). Additionally, there was a significant interaction in subjective vividness ratings by condition (F(2,30)=9.42; p=.003; Fig. 2D). Specifically, vividness ratings were significantly higher for object maintenance than static imagery (t(15)=3.71; p=.002), but not dynamic imagery trials (t(15)=1.71; p=.109). There was no difference in vividness ratings between dynamic and static imagery trials (t(15)=1.55; p=.143).

To summarize, performance, subjective memory, and vividness ratings were each significantly higher during object maintenance trials than static imagery trials, but not significantly different from dynamic imagery trials; and subjective memory ratings were significantly higher in dynamic imagery trials compared to static imagery trials.

Theta Power Changes and Source Reconstruction

To assess changes in frontal midline oscillatory power associated with the working memory task, we first extracted low frequency power spectra for the middle 18s of eyes-closed rest (i.e. baseline) and mental imagery of object location (i.e. delay) periods collapsed across all conditions from a 20 mm spherical ROI in source space, centered on frontal midline co-ordinates identified by a previous study (x: 0, y: 58, z: 22; Kaplan et al., 2014). A comparison of these power spectra identified a prominent increase in theta power between baseline and delay periods that peaked at ~5.5 Hz (Figure 3A). We subsequently defined our frontal midline theta band of interest as a 3Hz frequency window centred on this peak (i.e. 4-7 Hz). As expected, an examination of changes in 4-7 Hz power at the sensor level showed a large increase between

baseline and delay periods over frontotemporal regions (Figure 3B).

Next, we utilized the linearly constrained minimum variance (LCMV) beamformer algorithm (Barnes et al., 2003) to estimate all cortical sources that exhibited significant increases in 4-7 Hz theta power between baseline and delay periods. We identified a single large cluster peaking in the mPFC (peak at x: 22, y: 50, z: 0; t(15)=6.76; Z-score: 4.51; peak voxel FWE whole-brain corrected p=.012; Fig. 3C), extending into the right anterior temporal lobe / MTL. Using a 1x3 within-subject repeated measures ANOVA by condition, we did not observe any significant theta power differences between conditions. Furthermore, we observed no correlations between theta power and performance, retrieval phase reaction time, participant memory ratings, or vividness ratings over trials. Additionally, no cortical regions showed greater theta power during baseline periods, compared to the delay period.

Given that changes in the 1-4 Hz delta / low theta band have also been associated with human mnemonic function (Watrous et al., 2013; Jacobs, 2014), we used the LCMV beamformer algorithm to assay changes in 1-4 Hz power between baseline and delay periods across the whole brain. We observed a single subthreshold peak in the left insula that did not survive FWE correction for multiple comparisons. Notably, however, no significant changes were observed in the frontal or medial temporal lobes (data not shown).

Theta Phase Coupling

Next, we used the mPFC region that exhibited a significant theta power increase between baseline and delay periods as a seed region to investigate changes in theta phase coupling across the whole brain. As in past studies (Kaplan et al., 2014) the

specific seed voxel for each participant was chosen as that with the greatest theta power increase between baseline and delay periods within 20 mm of the group maximum, in order to account for variance in frontal midline theta source locations between participants (Ishihara et al., 1981).

First, we used the phase lag index (PLI; Stam et al., 2007; see Methods), a technique that eliminates volume conduction effects, to look for increases in theta phase coupling between the mPFC seed region and all other voxels in the brain. After correcting for eye movements and oscillatory power in seed and source voxels, we found no significant increases in theta phase coupling with the mPFC anywhere in the brain between delay and baseline periods averaged over all three conditions.

We then compared mPFC theta coupling differences between the three conditions using a 1x3 within-subject repeated measures ANOVA. In a whole-brain analysis, the most significant main effect of condition on mPFC phase-coupling was found in the left posterior MTL extending into the RSc (x: -28, y: -54, z: -2; Z-score: 4.13; F(2,30)=16.1; peak voxel FWE bilateral MTL small-volume corrected (SVC) p=.011; Fig 4A). Subsequent t-tests indicated that mPFC-MTL / RSc theta phase coupling was significantly higher for dynamic imagery than both object maintenance (x: -28, y: -54, z: -2; t(15)=4.60; Z-score: 3.97; peak voxel FWE SVC p=.016; Fig 4C) and static imagery (x:-30, y: -54, z: -4; t(15)=5.35; Z-score: 4.45; peak voxel FWE whole-brain corrected p=.03; Fig 4D).

To corroborate these findings we made use of a more sensitive measure of phase coupling – the phase-locking value (PLV: Lachaux et al., 1999; see Methods). We examined mPFC theta PLV within a 10 mm spherical ROI around the MTL / RSc peak voxel (x: -28, y: -54, z: -2) that displayed the most significant PLI difference between the

3 conditions above. Using a 1x3 repeated measures ANOVA, we observed the same main effect of condition ($F(2,30)=10.9$; $p=.001$). Subsequent paired t-tests revealed that dynamic imagery PLV was significantly higher than both static imagery ($t(15)=4.07$; $p=.001$) and object maintenance ($t(15)=3.54$; $p=.003$) within this region. As with the PLI analysis, we did not observe any significant differences in PLV between the static imagery and object maintenance conditions ($p>.05$).

Investigating possible MTL lateralization during dynamic imagery, we found no significant difference in mPFC theta coupling with left versus right posterior MTL during dynamic imagery when we compared PLI values in the left MTL region that showed a significant increase during dynamic imagery effect with those from the right MTL region (x: 48, y: -36, z: -10; $t(15)=4.75$; Z-score 3.67) that was most strongly coupled to the mPFC between baseline and delay periods. Crucially, we did not identify any other significant differences in theta phase coupling between mPFC any other brain regions or between any other conditions.

In order to ascertain whether mPFC-posterior MTL theta phase coupling difference between conditions related to differences in performance measures across conditions, we tested whether the mPFC-posterior MTL theta PLI values across all delay period trials correlated with our four behavioral regressors across trials. Using a 10 mm sphere around the left posterior MTL PLI peak, we found no significant correlations (all $p>.05$) with any of the four behavioral regressors: memory performance, reaction time, subjective memory, and vividness ratings. Lastly, we investigated whether mPFC mean PLI differences between delay and baseline periods in any other brain regions correlated with any of these performance measures across trials, but did not identify any significant effects.

Discussion

We have identified an increase in mPFC and anterior / medial temporal lobe theta power during eyes-closed mental imagery of previously learned object sequences during a spatial working memory delay period compared to a preceding baseline period of eyes closed rest. We found that the mPFC theta rhythm showed significantly stronger coupling with the left posterior MTL / RSc than any other brain region during imagined movement around learned object locations (dynamic imagery), compared to static imagery of learned object sequences in a scene (static imagery), or over a blank background (object maintenance).

Our theta power findings add to a rich literature of human working memory studies exploring theta oscillations in the frontal midline during the delay period of human working memory tasks (see Hsieh & Ranganath, 2014 for a review). We found increased mPFC theta power for mental imagery during a working memory delay period prior to retrieval, versus a baseline period, which parallels results from a previous MEG study that found increased mPFC theta during cued retrieval of previously learned spatial representations (Kaplan et al., 2014). Furthermore, similar to previous MEG and intracranial EEG studies, we also observed increased MTL theta power during a working memory delay period (Tesche et al., 2000; Raghavachari et al., 2006; Cashdollar et al., 2009; Axmacher et al., 2010; Poch et al., 2011). Frontal midline theta is often linked to directed attention (Ishii et al., 1999, 2014; see review by Mitchell et al., 2008), which we did not directly measure in this task. However, if there were any differences in directed attention between conditions, they did not cause any observable differences in frontal midline theta power .

Specifically comparable to our findings, a previous study observed increased delay period mPFC and hippocampal theta power during spatial integration of object locations (Olsen et al., 2013). Unlike the study by Olsen and colleagues, we did not observe separate theta sources in the mPFC and hippocampus during the delay period. This discrepancy might be a consequence of the relatively small number of trials and participants in our task, which increases the difficulty of estimating deep sources with MEG (Quraan et al., 2011; also see Dalal et al., 2013 for evidence relating direct human hippocampal recordings to MEG source reconstruction). In addition, EEG studies have seen increased frontal midline theta oscillations corresponding to the maintenance of the serial position of items (Hsieh et al., 2011), both spatial location and temporal order judgements (Roberts et al., 2013), and the number of items being maintained in working memory (Jensen & Tesche, 2002). These results allow for the possibility that the frontal midline theta rhythm might provide top-down control in order to maintain the serial order or relation between previously learned spatial or temporal hippocampal representations prior to retrieval (Olsen et al., 2013), which in the case of our spatial imagery task would also require MTL / parietal regions related to processing different viewpoints (Byrne et al., 2007).

The mPFC delay period theta rhythm was more strongly coupled to the posterior MTL than any other brain region, further emphasizing the importance of mPFC-MTL theta phase coupling during mnemonic tasks (Anderson et al., 2010; Guitart-Masip et al., 2013; Watrous et al., 2013; Fuentemilla et al., 2014; Kaplan et al., 2014; Garrido et al., 2015; Backus et al., 2016). Although the mPFC-right posterior MTL phase coupling delay period effect did not significantly vary by condition, unlike the mPFC-left MTL theta coupling effect we observed, all delay period conditions were also above baseline.

Looking across the different imagery conditions revealed significant differences in mPFC theta phase coupling with the left posterior MTL / RSc according to condition. Crucially, mPFC-MTL / RSc theta coupling was higher for dynamic spatial imagery than our other two delay period imagery manipulations and the mPFC theta rhythm displayed no significant 4-7 Hz phase-locking with any other brain region. We also found that mPFC-MTL theta coupling did not show any effect of hemispheric lateralization for dynamic imagery, since there was no significant mPFC theta coupling with left or right MTL during dynamic imagery. Crucially, no behavioral rating correlated with mPFC-pMTL / RSc theta coupling between the three conditions, suggesting that the increase in mPFC-pMTL / RSc theta coupling for dynamic imagery was due to specific condition demands (e.g. mental imagery for multiple viewpoints, dynamically changing scenes) rather than differences in general behavioral performance (e.g. memory strength). Similar to past studies of spatial attention in human electrophysiology (Mangun & Hillyard, 1990), future experiments should investigate the relationships between distributed neural responses at different stages of dynamic spatial imagery and measures of performance or vividness, to separate responses reflecting the types of processing involved from those reflecting successful execution of that processing type. Furthermore, human intracranial EEG recordings may be better suited than MEG studies to investigate the temporal dynamics of interregional phase interactions and future studies can investigate the potentially rich temporal phase coupling dynamics that might differ between imagery conditions.

Notably, one intracranial EEG study recording from human MTL and RSc (Foster et al., 2013) found increased theta phase coupling between the two regions during autobiographical memory, an effect that might be due to the increased dynamic imagery

demands of the task. Taken together, these findings complement a previous hypothesis that theta synchronization between MTL / RSc and mPFC should accompany increased contextual associations (Aminoff et al., 2013). Both the posterior MTL and RSc are thought to encode different viewpoints into a large-scale understanding of an environment (Vass & Epstein, 2013).

In terms of specific neural mechanisms, the finding of mPFC-MTL / RSc theta synchrony during dynamic imagery (i.e. movement of viewpoint) supports a recent model of spatial mental imagery. This model proposes that coherent spatial imagery results from a theta-rhythmic interaction between MTL and medial parietal areas, mediated by RSc (Byrne et al., 2007; Burgess et al., 2001). Within this model, prefrontal cortex is hypothesized to control movements of viewpoint during mental exploration, by modulating alternating temporal-parietal flows of information (Dhindsa et al. 2014).

Our findings illustrate the importance of mPFC-MTL interregional phase coupling in memory, irrespective of the presence or absence of theta power changes (Watrous et al., 2013; Brincat & Miller, 2015). We provide further support to an expanding literature relating frequency band–specific interregional phase coupling to a variety of cognitive processes (for reviews see Fries, 2005; Buzsáki, 2006; Jutras & Buffalo, 2010; Fell & Axmacher, 2011). An important caveat to our findings is that our 4-7 Hz dynamic imagery effect is localized to the posterior MTL / RSc, not specifically to the hippocampus. Indeed, a lower frequency ~1-4 Hz in the human hippocampus has been related to the hippocampal theta rhythm in rodents (Watrous et al., 2013; Jacobs, 2014) and we had no prediction about how other frontal midline or hippocampal theta rhythms might couple with other frequency bands in other neocortical regions, such as the alpha / beta band, that are present during memory formation (Hanslmayr et al.,

2016). Future models can investigate interregional interactions and potential oscillatory multiplexing (Ekstrom & Watrous, 2014; Watrous & Ekstrom, 2014) in order to better explore the mechanisms underlying dynamic imagery and memory formation.

Hippocampal-mPFC theta phase-locking is also commonly observed during rodent spatial exploration and correlates with behavioral performance (Jones & Wilson, 2005; Benchenane et al., 2010; Hyman et al., 2010; Sigurdsson et al., 2010; see Colgin, 2011 and Gordon, 2011 for reviews). Notably, grid cell firing in the entorhinal cortex is also associated with theta states and grid-like processing has been observed in medial prefrontal, parietal and temporal regions (Doeller et al., 2010). Recent fMRI studies found grid-like processing in the MTL also during mental navigation (Bellmund et al., 2016; Horner et al., 2016), which parallels our dynamic versus static imagery results and suggests that both theta rhythmicity and spatial cell firing might play a role in mental exploration of imagined spaces.

Conclusions

Our findings suggest that theta oscillations in the mPFC and MTL could work in tandem, along with the RSc, to coordinate dynamic mental imagery during spatial working memory maintenance. Our results allow for the possibility that oscillatory interactions in the theta band between mPFC and the MTL / RSc in humans could underlie the mental exploration of possible spatial trajectories and, more generally, mental simulation and fictive planning (Byrne et al., 2007; Buzsáki & Moser, 2013).

References

Aftanas LI, Golocheikine SA (2001) Human anterior and frontal midline theta and lower alpha reflect emotionally positive state and internalized attention: high-resolution EEG investigation of meditation. Neurosci Lett. **310**:57-60.

Aminoff EM, Kveraga K, Bar M (2013) The role of the parahippocampal cortex in cognition. Trends Cog Sci **17**:379-90

Anderson KL, Rajagovindan R, Ghacibeh GA, Meador KJ, Ding M (2010) Theta oscillations mediate interaction between prefrontal cortex and medial temporal lobe in human memory. Cereb Cortex **20**:1604-12.

Axmacher N, Henseler MM, Jensen O, Weinrech I, Elger CE, Fell J (2010) Cross-frequency coupling supports multi-item working memory in the human hippocampus. Proc Natl Acad Sci U.S.A **107**:3228-33

Backus AR, Schoffelen JM, Szebényi S, Hanslmayr S, Doeller CF (2016) Hippocampal-Prefrontal Theta Oscillations Support Memory Integration. Curr Biol **26**:450-7.

Banquet JP (1973) Spectral analysis of the EEG in meditation. Electroencephalogr. Clin. Neurophysiol. **35**:143-51.

Barnes GR, Hillebrand A. 2003. Statistical flattening of MEG beamformer images. Hum Brain Mapp **18**:1–12.

Battaglia FP, Benchenane K, Sirota A, Pennartz CM, Wiener SI (2011) The hippocampus: hub of brain network communication for memory. Trends Cogn Sci **15**:310–318

Bellmund JL, Deuker L, Navarro Schröder T, Doeller CF (2016) Grid-cell representations in mental simulation. Elife **5**:e17089.

Benchenane K, Peyrache A, Khamassi M, Tierney PL, Gioanni Y, Battaglia FP, Wiener SI (2010) Coherent theta oscillations and reorganization of spike timing in the hippocampal-prefrontal network upon learning. Neuron **66**:921-36.

Bird CM, Burgess N (2008) The hippocampus and memory: insights from spatial processing. Nat Rev Neurosci **9**:182-94.

Brincat SL, Miller EK (2015) Frequency-specific hippocampal-prefrontal interactions during associative learning. Nat Neurosci **18:**576-81.

Burgess N, Becker S, King JA, O'Keefe J (2001) Memory for events and their spatial context: models and experiments, Philos. Trans. R. Soc. Lond B. **356**:1493-1503.

Burgess N, Spiers HJ, Paleologou E (2004) Orientational manoeuvres in the dark: dissociating allocentric and egocentric influences on spatial memory. Cognition **94**:149-

66.

Burgess N (2006) Spatial memory: how egocentric and allocentric combine. Trends Cogn Sci **10**:551-7.

Buzsáki G (2006) Rhythms of the Brain, Oxford Univ. Press, New York

Buzsáki G, Moser EI (2013) Memory, navigation and theta rhythm in the hippocampal-entorhinal system. Nat Neurosci **16**:130-8.

Byrne P, Becker S, Burgess N (2007) Remembering the past and imagining the future: a neural model of spatial memory and imagery. Psychol Rev **114**(2):340-75.

Caplan JB, Madsen JR, Schulze-Bonhage A, Aschenbrenner-Scheibe R, Newman EL, Kahana MJ (2003) Human theta oscillations related to sensorimotor integration and spatial learning. J Neurosci **23**:4726-36.

Cashdollar N, Malecki U, Rugg-Gunn FJ, Duncan JS, Lavie N, Duzel E (2009) Hippocampus-dependent and –independent theta-networks of active maintenance. Proc Natl Acad Sci U.S.A. **106**:20493-98.

Colgin LL (2011) Oscillations and hippocampal-prefrontal synchrony. Curr Opin Neurobiol **21**:467-74.

Dalal SS, Jerbi K, Bertrand O, Adam C, Ducorps A, Schwartz D, Garnero L, Baillet S, Martinerie J, Lachaux J-P (2013) Evidence for MEG detection of hippocampus oscillations and cortical gamma-band activity from simultaneous intracranial EEG. *Epilepsy Behav*. **28**:288-92.

Dhindsa K, Drobinin, King J, Hall GB, Burgess N, Becker S (2014) Examining the role of the temporo-parietal network in memory, imagery, and viewpoint transformations. Front Hum Neurosci **8**:709

Doeller CF, Barry C, Burgess N (2010) Evidence for grid cells in a human memory network. Nature 463:657-61.

Ekstrom AD, Caplan JB, Ho E, Shattuck K, Fried I, Kahana MJ (2005) Human hippocampal theta activity during virtual navigation. Hippocampus **15**:881-9.

Ekstrom AD, Watrous AJ (2014) Multifaceted roles for low-frequency oscillations in bottom-up and top-down processing during navigation and memory. Neuroimage **85**:667-77.

Epstein RA (2008) Parahippocampal and retrosplenial contributions to human spatial navigation. Trends Cogn Sci. **12**:388-96.

Fell J, Axmacher N (2011) The role of phase synchronization in memory processes. Nat Rev Neurosci **12**:105-18.

Foster BL, Kaveh A, Dastjerdi M, Miller KJ, Parvizi J (2013) Human retrosplenial cortex displays transient theta phase locking with medial temporal cortex prior to activation during autobiographical memory retrieval. J Neurosci **33**:10439-46.

Fries P (2005) A mechanism for cognitive dynamics: neuronal communication through neuronal coherence. Trends Cogn Sci **9**:474-80.

Fuentemilla L, Barnes GR, Duzel E, Levine B (2014) Theta oscillations orchestrate medial temporal lobe and neocortex in remembering autobiographical memories. Neuroimage **85**:730-7.

Garrido MI, Barnes GR, Kumaran D, Maguire EA, Dolan RJ (2015) Ventromedial prefrontal cortex drives hippocampal theta oscillations induced by mismatch computations. Neuroimage **15**:362-70.

Gordon JA (2011) Oscillations and hippocampal-prefrontal synchrony. Curr Opin Neurobiol **21**:486-91.

Graziano M, Gross C (1993) A bimodal map of space: somatosensory receptive fields in the macaque putamen with corresponding visual receptive fields. *Experimental Brain Research* **97**:96-109.

Guitart-Masip M, Barnes GR, Horner A, Bauer M, Dolan RJ, Duzel E (2013) Synchronization of medial temporal lobe and prefrontal rhythms in human decision making. J Neurosci **33**:442-51.

Hanslmayr S, Staresina BP, Bowman H (2016) Oscillations and Episodic Memory: Addressing the Synchronization/Desynchronization Conundrum. Trends Neurosci. **39**:16-25.

Hassabis D, Kumaran D, Vann SD, Maguire EA (2007) Patients with hippocampal amnesia cannot imagine new experiences. Proc Natl Acad Sci USA **104**:1726-31.

Henson RN, Mattout J Phillips C, Friston KJ (2009) Selecting forward models for MEG source-reconstruction using model-evidence. Neuroimage 46:168-76.

Horner AJ, Bisby JA, Zotow E, Bush D, Burgess N (2016) Grid-like Processing of Imagined Navigation. Curr Biol **26**:842-7.

Hsieh LT, Ekstrom AD, Ranganath C (2011) Neural oscillations associated with item and temporal order maintenance in working memory. J Neurosci **31**:10803-10.

Hsieh LT, Ranganath C (2014) Frontal midline theta oscillations during working memory maintenance and episodic encoding and retrieval. Neuroimage **85**:721-9.

Hyman JM, Zilli EA, Paley AM, Hasselmo ME (2010) Working Memory Performance Correlates with Prefrontal-Hippocampal Theta Interactions but not with Prefrontal Neuron Firing Rates. Front Integr Neurosci **4**:2.

Ishii R, Shinosaki K, Ukai S, Inouye T, Ishiahara T, Yoshimine T, Hirabuki N, Asada H, Kihara T, Robinson SE, Takeda M (1999) Medial prefrontal cortex generates frontal midline theta rhythm. Neuroreport **10**:675-9.

Ishii R, Canuet L, Ishihara T, Aoki Y, Ikeda S, Hata M, Katsimichas T, Gunji A, Takahashi H, Nakahachi T, Iwase M, Takeda M (2014) Frontal midline theta rhythm and gamma power changes during focused attention on mental calculation: an MEG beamformer analysis. Front Hum Neurosci **8**:406

Isihara T, Hayashi H, Hishikawa Y (1981) Distribution of frontal midline theta rhythm (FmO) on the scalp in different states (mental calculation, resting and drowsiness). Electroencephalogr. Clin Neurophysiol. **52**,S19.

Jacobs J (2014) Hippocampal theta oscillations are slower in humans than in rodents: implications for models of spatial navigation and memory. Philos Trans R Soc Lond B Biol Sci **369**:20130304.

Jensen O, Tesche CD (2002) Frontal theta activity in humans increases with memory load in a working memory task. Eur J Neurosci **28**:67-72.

Jones MW, Wilson MA (2005) Theta rhythms coordinate hippocampal-prefrontal interactions in a spatial memory task. PLoS Biol e402.

Jutras MJ, Buffalo EA (2010) Synchronous neural activity and memory formation. Curr Opin Neurobiol **20**:150-5.

Kahana MJ, Sekuler R, Caplan JB, Kirschen M, Madsen JR (1999) Human theta oscillations exhibit task dependence during virtual maze navigation. Nature **399**:781-4.

Kaplan R, Doeller CF, Barnes GR, Litvak V, Düzel E, Bandettini PA, Burgess N (2012) Movement-related theta rhythm in humans coordinating self-directed hippocampal learning. PLoS Biol **10**:e1001267.

Kaplan R, Bush D, Bonnefond M, Bandettini PA, Barnes GR, Doeller CF, Burgess N (2014) Medial prefrontal phase coupling during spatial memory retrieval. Hippocampus **24**:656-65.

Kiebel SJ, Friston KJ (2004a) Statistical parametric mapping for event-related potentials: 1. Generic considerations. Neuroimage **22**:492-502.

Kiebel SJ, Friston KJ (2004b) Statistical parametric mapping for event-related potentials (II): a hierarchical temporal model. Neuroimage **22**:503-520.

Kilner JM, Kiebel SJ, Friston KJ (2005). Applications of random field theory to electrophysiology. Neuroscience Letters **374**:174-78.

Lachaux J, Rodriguez E, Martiniere J, Varela F (1999). Measuring phase synchrony in brain signals. Hum Brain Mapp **8**:194–208.

Lehmann D, Henggeler B, Koukkou M, Michel CM (1993) Source localization of brain electric field frequency bands during conscious, spontaneous, visual imagery and abstract thought. Brain Res. Cogn. Brain Res. **1**:203-10.

Litvak V, Mattout J, Kiebel S, Phillips C, Henson R, Kilner J, Barnes G, Oostenveld R, Daunizeau J, Flandin G, Penny W, Friston K (2011) EEG and MEG data analysis in SPM8. Comput Intell Neurosci **2011**:852961.

Mangun GR, Hillyard SA (1990) Allocation of visual attention to spatial locations: tradeoff functions for event-related brain potentials and detection performance. Percept Psychophys. **47**:532-50.

Marchette SA, Vass LK, Ryan J, Epstein RA (2014) Anchoring the neural compass: coding of local spatial reference frames in human medial parietal lobe. Nat Neurosci **17**:1598-606.

Mitchell DJ, McNaughton N, Flanagan D, Kirk IJ. (2008) Frontal-midline theta from the perspective of hippocampal "theta". Prog Neurobiol **86**:156-85.

Muthukumaraswamy SD, Singh KD. (2011) A cautionary note on the interpretation of phase-locking estimates with concurrent changes in power. Clin Neurophysiol **122**:2324-2325.

Nolte G. 2003. The magnetic lead field theorem in the quasi-static approximation and its use for magnetoencephalography forward calculation in realistic volume conductor. Phys Med Biol **48**:3637–3652.

O'Keefe J, Nadel L Hippocampus as a Cognitive Map. New York. Oxford UP; 1978.

O'Keefe J (2006) Hippocampal neurophysiology in the behaving animal. In: Andersen P, Morris R. M, Amaral D. G, Bliss T. V. P, O'Keefe J, editors. The hippocampus book. New York: Oxford University Press. pp. 475–548.

O'Neill PK, Gordon JA, Sigurdsson T (2013) Theta oscillations in the medial prefrontal cortex are modulated by spatial working memory and synchronize with the hippocampus through its ventral subregion. J Neurosci **33**:14211-24

Olsen RK, Rondina Ii R., Riggs L, Meltzer JA, Ryan JD (2013) Hippocampal and neocortical oscillatory contributions to visuospatial binding and comparison. Journal of Experimental Psychology: General **142**:1335-45.

Oostenveld R, Fries P, Maris E, Schoffelen J-M. 2011. FieldTrip: Open source software for advanced analysis of MEG, EEG, and invasive electrophysiological data. Comput Intell Neurosci **2011**:156869.

Poch C, Fuentemilla L, Barnes GR, Duzel E (2011) Hippocampal theta-phase modulation of replay correlates with configural-relational short-term memory performance. J Neurosci **31**:7-38-42

Quraan MA, Moses SN, Hung Y, Mills T, Taylor MJ (2011) Detection and localization of hippocampal activity using beamformers with MEG: a detailed investigation using simulations and empirical data. Hum. Brain Mapp. **32**:812-27.

Raghavachari S, Lisman JE, Tully M, Madsen JR, Bromfield EB, Kahana MJ (2006) Theta oscillations in human cortex during a working-memory task: evidence for local generators. J Neurophysiol **95**:1630-8

Roberts BM, Hsieh LT, Ranganath C (2013) Oscillatory activity during maintenance of spatial and temporal information in working memory. Neuropsychologia **51:**349-57.

Sasaki K, Nambu A, Tsujimoto T, Matsuzaki R, Kyuhou S, Gemba H (1996) Studies on integrative functions of the human frontal association cortex with MEG. Cogn. Brain Res **5**:165-74.

Sauseng P, Klimesch W, Doppelmayr M, Hanslmayr S, Schabus M, Gruber WR (2004) Theta coupling in the human electroencephalogram during a working memory task. Neurosci Lett **354**:123-6.

Schacter DL, Addis DR, Hassabis D, Martin VC, Spreng RN, Szpunar KK (2012) The future of memory: remembering, imagining, and the brain. Neuron **76**:677-94

Sigurdsson T, Stark KL, Karayiorgou M, Gogos JA, Gordon JA (2010) Impaired hippocampal-prefrontal synchrony in a genetic mouse model of schizophrenia. Nature **464**:763-767.

Stam CJ, Nolte G, Daffertshofer A. 2007. Phase lag index: Assessment of functional connectivity from multi channel EEG and MEG with diminished bias from common sources. *Hum Brain Mapp* **28**:1178–1193.

Tesche CD, Karhu J (2000) Theta oscillations index human hippocampal activation during a working memory task. Proc Natl Acad Sci U S A **97**:919-24

Troebinger L, Lopez JD, Lutti A, Bradbury D, Bestmann S, Barnes G (2014). High precision anatomy for MEG. Neuroimage 86:583-91.

Tzourio-Mazoyer N, Landeau B, Papathanassiou D, Crivello F, Etard O, Delroix N, Mazoyer B, Joliot M. 2002. Automated anatomical labelling of activations in SPM using a macroscopic anatomical parcellation of the MNI MRI single-subject brain. *Neuroimage* **15**:273–289.

Vanderwolf CH (1969) Hippocampal electrical activity and voluntary movement in the rat. Electroencephalogr Clin Neurophysiol **26**:407-18.

Vass LK, Epstein RA (2013) Abstract representations of location and facing direction in the human brain. J Neurosci **33**:6133-42.

Wang RF, Simons DJ (1999) Active and passive scene recognition across views. Cognition **70**:191-210.

Wang RF, Spelke ES (2000) Updating egocentric representations in human navigation. Cognition **77**:215-50.

Watrous AJ, Lee DJ, Izadi A, Gurkoff GG, Shahlaie K, Ekstrom AD (2013) A comparative study of human and rat hippocampal low-frequency oscillations during spatial navigation. Hippocampus **23**:656-61.

Watrous AJ, Tandon N, Conner CR, Pieters T, Ekstrom AD (2013) Frequency-specific network connectivity increases underlie accurate spatiotemporal memory retrieval. Nat Neurosci **16**:349-56.

Watrous AJ, Ekstrom AD (2014) The spectro-contextual encoding and retrieval theory of episodic memory. Front Hum Neurosci. **8**:75.

Worsley KJ, Marrett S, Neelin P, Vandal AC, Friston KJ, Evans AC (1996) A unified statistical approach for determining significant signals in images of cerebral activation. Hum Brain Mapp **4**:58-73

Worsley KJ, Taylor JE, Tomaiuolo F, Lerch J (2004) Unified univariate and multivariate random field theory. *Neuroimage* **23**(Supp 1):S189-S195.

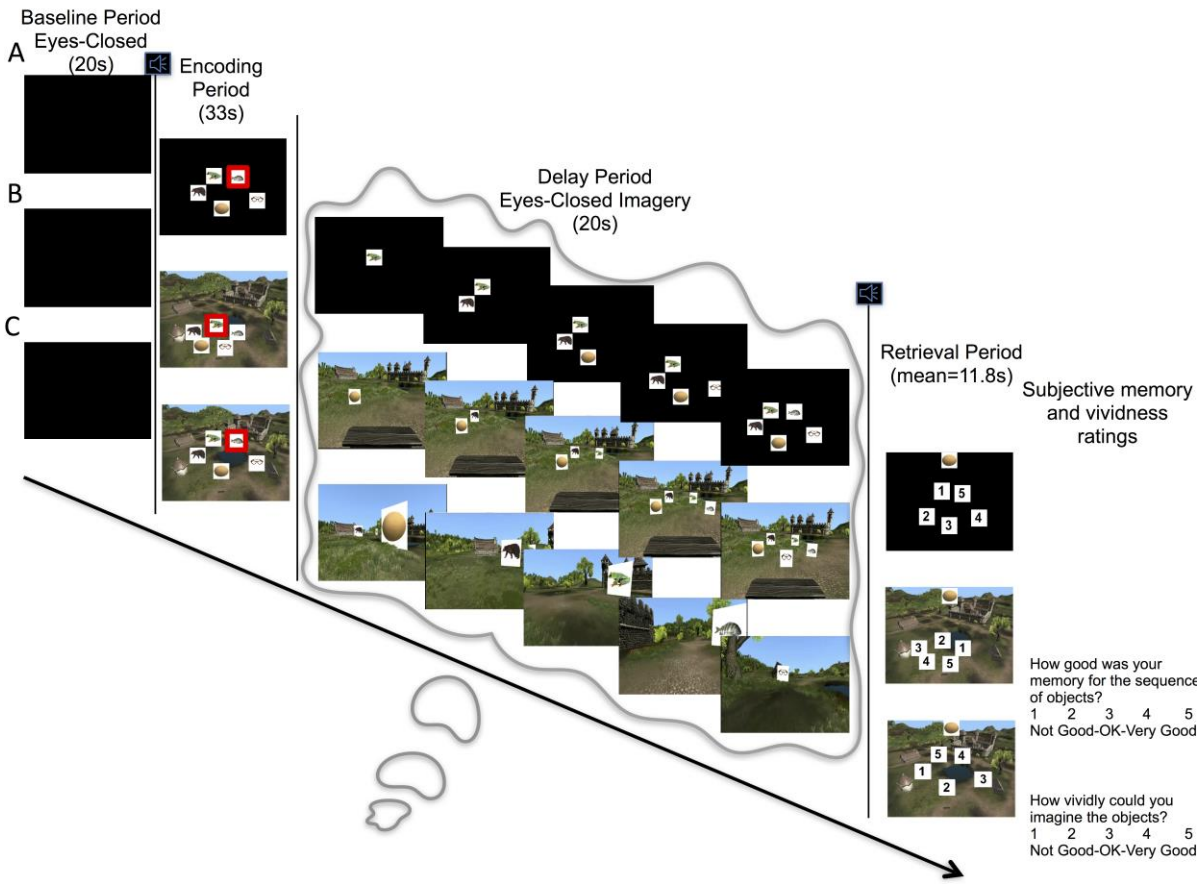

Figure 1. Experiment Trial Structure. After a 20s eyes-closed baseline period, an auditory tone alerted participants to an upcoming encoding period (for all trial types). These encoding periods fell into one of three conditions. A. Object maintenance. Participants were presented with a set of objects overlaid on a black background and instructed to maintain a memory of those object locations during a 20s eyes-closed delay period. B. Static imagery. Participants were presented with a set of objects overlaid on a static scene and instructed to maintain a memory of those object locations from an imagined first-person viewpoint sitting on the bench set within each scene during a 20s eyes-closed delay period. C. Dynamic imagery. Participants were presented with a set of objects overlaid on a static scene and instructed to maintain a memory of those object locations from a first-person viewpoint as they imagined moving through the scene on a trajectory that sequentially passed each object during a 20s eyes-closed delay period. After the delay period, participants were prompted with an image of each object and asked to identify its previous location at their own pace (mean=11.8s), as well as report their perceived memory performance and vividness of imagination during the delay period.

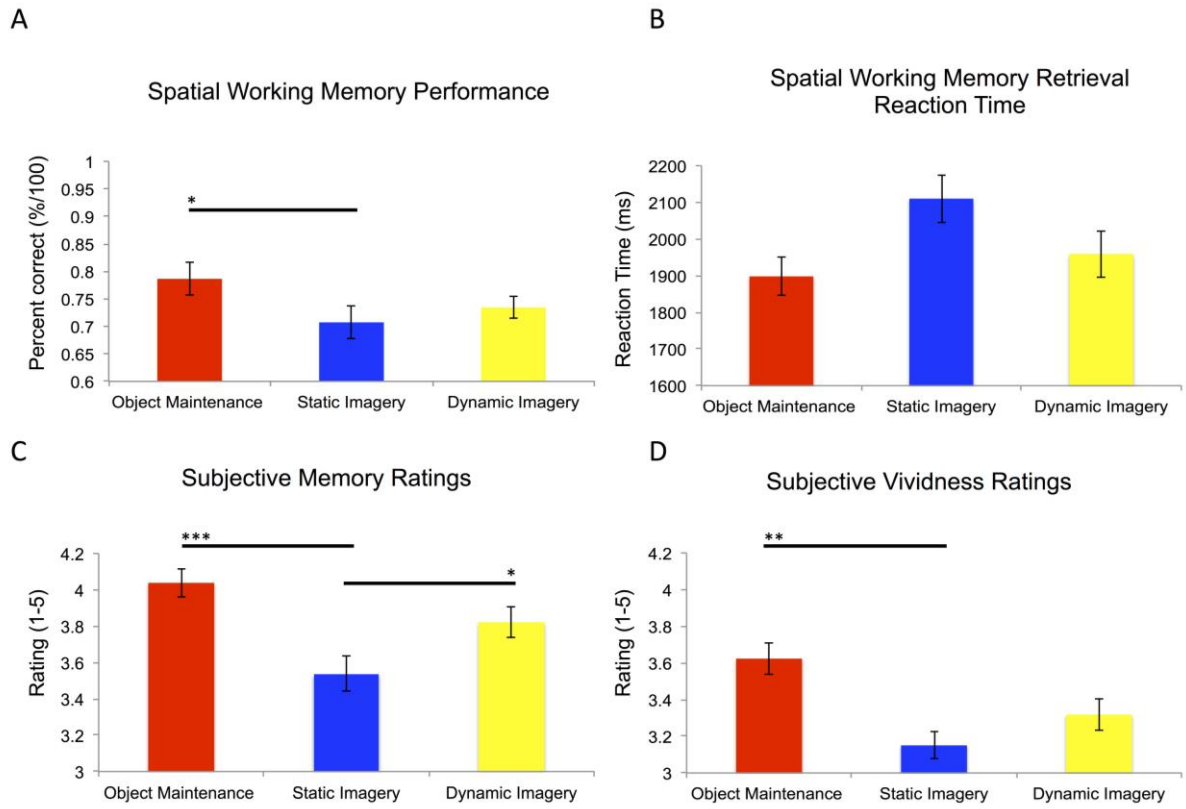

Figure 2: Behavioral Results. A: Average trial-by-trial memory performance for each experimental condition during the retrieval phase. Main effect of condition: $F(2,30)=5.66$, $p=.016$. B: Average trial-by-trial reaction time during the retrieval phase for objects 2-5 in the sequence (as retrieval was self-paced, and very long reaction times were often recorded for object 1). C: Average trial-by-trial subjective memory ratings made on a scale of 1-5 (1=unsatisfactory; 5=very good) given immediately following the retrieval phase. Main effect of condition: $F(2,30)=11.4$, $p=.001$. D: Average trial-by-trial vividness ratings made on a scale 1-5 (1=poor; 5=very good). Main effect of condition: $F(2,30)=9.42$, $p=.003$. All bar graphs show mean ± SEM over the 16 participants). *=p<.05;**=p<.005;***=p<.001

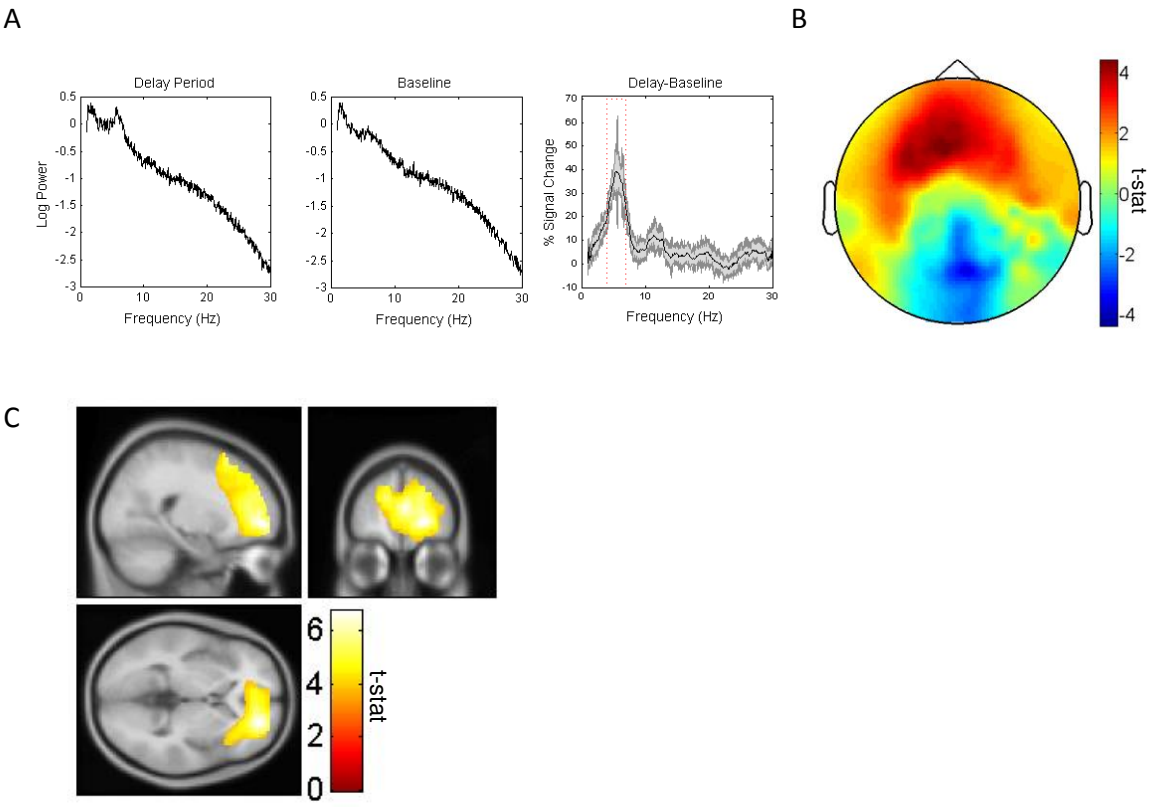

Figure 3. Delay versus baseline period 4-7 Hz theta power changes. A. Power spectra from a virtual electrode placed in the frontal midline region identified by a previous study (x:0, y: 58, z: 22; Kaplan et al., 2014) for delay and baseline periods, as well as the difference in power between the two, averaged across all trials and participants. The power difference plot shows mean ± SEM across participants in gray. The power difference spectra shows a single prominent peak at ~5.5Hz, and we focus our subsequent analyses on a 3Hz frequency band centred on this peak (i.e. 4-7Hz). B. Scalp-level delay versus baseline period 4-7 Hz theta power changes, which show an increase across the frontal midline region. C. Left: Medial prefrontal cortex (x: 22, y: 50, z: 0; Z-score: 4.51; peak voxel family-wise error (FWE) corrected for the whole brain volume p=.012) theta power changes between the baseline and delay periods. Image shown at p<.001 uncorrected and overlaid on the canonical Montreal Neurological Institute 152 T1 image.

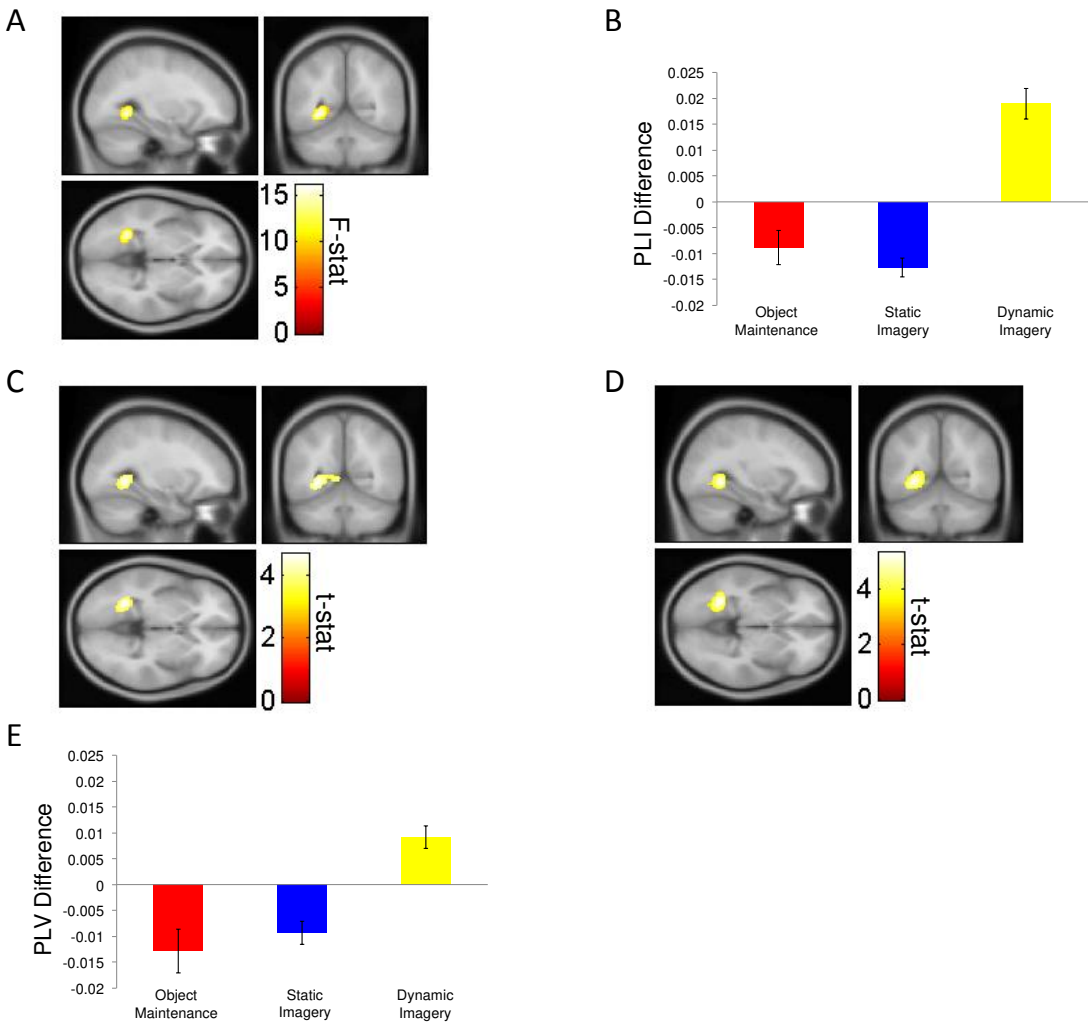

Figure 4. Delay period 4-7 Hz mPFC theta phase coupling; phase-lag index (PLI) whole-brain analysis A. 1x3 interaction between object maintenance, static imagery, and dynamic imagery for mPFC theta phase-coupling, showing a significant cluster in the left posterior medial temporal lobe (MTLx: -28, y: -54, z: -2; Z-score: 4.13; peak voxel FWE for bilateral MTL p=.011) extending into the retrosplenial cortex (RSc). B. Mean mPFC PLI with 10 mm sphere around the left posterior MTL peak voxel (x:-28, y: -54, z: -2) for all three conditions versus baseline. C. mPFC theta phase-coupling for dynamic imagery versus object maintenance, showing a significant cluster in the left posterior MTL (x: -28, y: -54, z: -2; Z-score: 3.97; peak voxel FWE for bilateral MTL p=.016), extending into the RSc. D. mPFC theta phase-coupling for dynamic imagery versus static imagery, showing a significant cluster in the left posterior MTL (x:-30, y: -54, z: -4; Z-score: 4.45; peak voxel FWE corrected for whole-brain volume p=.03), extending into the RSc. All images shown at p<.001 uncorrected for visualization purposes and overlaid on the canonical Montreal Neurological Institute 152 T1 image. E. Mean mPFC phase-locking value (PLV) with 10 mm sphere around the left posterior MTL peak PLI voxel in 4A for all three conditions versus baseline. All bar graphs show mean ± SEM over the 16 participants.